



**HAL**  
open science

# Epoxy homopolymerization as a tool to tune thermomechanical properties and fracture toughness of vitrimer

Kanokporn Tangthana-Umrung, Quentin Arthur Poutrel, Matthieu Gresil,  
Quentin Arthur Poutrel

## ► To cite this version:

Kanokporn Tangthana-Umrung, Quentin Arthur Poutrel, Matthieu Gresil, Quentin Arthur Poutrel. Epoxy homopolymerization as a tool to tune thermomechanical properties and fracture toughness of vitrimer. *Macromolecules*, 2021, 54 (18), pp.8393-8406. 10.1021/acs.macromol.1c00861 . hal-03370809

**HAL Id: hal-03370809**

**<https://hal.science/hal-03370809>**

Submitted on 8 Oct 2021

**HAL** is a multi-disciplinary open access archive for the deposit and dissemination of scientific research documents, whether they are published or not. The documents may come from teaching and research institutions in France or abroad, or from public or private research centers.

L'archive ouverte pluridisciplinaire **HAL**, est destinée au dépôt et à la diffusion de documents scientifiques de niveau recherche, publiés ou non, émanant des établissements d'enseignement et de recherche français ou étrangers, des laboratoires publics ou privés.

# Epoxy homopolymerization as a tool to tune thermo-mechanical properties and fracture toughness of vitrimer

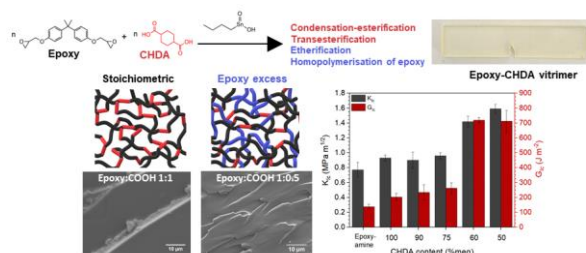
*Kanokporn Tangthana-umrung<sup>1</sup>, Quentin Arthur Poutrel<sup>2</sup> and Matthieu Gresil<sup>3\*</sup>*

<sup>1</sup>Department of Materials, University of Manchester, UK

<sup>2</sup>Molecular, Macromolecular Chemistry, and Materials, ESPCI Paris, PSL University, CNRS, 10 rue Vauquelin, 75005 Paris, France

<sup>3</sup>i-Composites Lab, Department of Material Science and Engineering, Department of Mechanical and Aerospace Engineering, Monash University, Wellington Rd, Clayton VIC 3800, Australia

Keywords: Epoxy vitrimer, Covalent adaptable networks, Transesterification, Fracture toughness



“For Table of Contents use only”

**ABSTRACT:** Epoxy-dicarboxylic acid vitrimer was prepared by solvent-free reaction of diglycidyl ether of bisphenol A (DGEBA) and 1,4-cyclohexane dicarboxylic acid (CHDA) with the addition of monobutyltin oxide (Sn) as catalyst. By tailoring the catalyst content ( $\geq 5$  mol%), an effective conversion of functional groups during cure demonstrated the network polymerization mechanisms and a sequence of the side reactions. Indeed, the manufactured vitrimers exhibit creep and full stress relaxation thanks to catalytic transesterifications. By changing the epoxy:diacid ratio, thermo-mechanical properties and mechanical behavior of the epoxy-acid vitrimers can be tuned while keeping self-healing ability. At high epoxy excess, both glass transition temperature ( $T_g$ ) and solid-liquid viscoelastic transition temperature ( $T_v$ ) shift to higher temperature. At vitrimer formulation 1:0.6 and 1:0.5 (epoxy:acyl), remarkable improvement of fracture toughness ( $K_{Ic}$ ) is observed, indicating the transition from stiff to relatively ductile materials at 1:0.6. This is attributed to the altered network structures due to etherification and epoxy homopolymerization. The rough fracture surface suggests more energy dissipation during crack propagation in vitrimer with high excess epoxy. After healing, welded vitrimers still exhibit good fracture toughness with only slight reduction ( $<10\%$ ) in  $K_{Ic}$ . We believe that these vitrimer formulations are promising as matrices in the composite fields.

## INTRODUCTION

Thermosetting epoxy resin exhibits remarkable properties including high strength, good thermal properties, excellent dimensional stability, and chemical resistance due to their 3D cross-linked structure.<sup>1</sup> Usages of this type of thermoset covers several applications such as coating, adhesive, energy, medical, civil, automotive, and aerospace.<sup>2,3</sup> However, conventional epoxies lack of reprocessability due to their permanent crosslink. To overcome these drawbacks, the concept of thermosets comprised of exchangeable bonds was developed, namely, covalent adaptable networks (CANs).<sup>4</sup> The dynamic covalent reactions (either associative or dissociative<sup>4,5</sup>) allow to rearrange the network topology of the crosslinked polymer. In 2011, Leibler and co-workers introduced transesterification reactions by addition of catalyst in cured epoxy-anhydride and epoxy-diacid formulations. The materials were named “vitrimers”,<sup>6</sup> and two main transitions were found in these materials: (i) the glass transition temperature ( $T_g$ ) and, the freezing topology temperature ( $T_v$ ).<sup>7</sup> The associative bond exchange reaction (BER) used (*i.e.* transesterification) allows vitrimers to relax stress and flow without losing the crosslink density or network connectivity.<sup>8</sup> Viscosity of material decrease concomitantly with temperature increase, following an Arrhenius’ law. These properties lead the material to be reprocessable while keeping similar behavior of conventional epoxy thermoset at service temperature (*i.e.* below  $T_v$ ).

In recent years, understanding of vitrimer networks was intensively investigated in several aspects. A number of theoretical studies developed models such as a continuum model<sup>9</sup>, a coarse-grained mode<sup>10</sup> and first-principles mode-coupling theory<sup>10,11</sup>, aiming to link microstructure properties and dynamic network of vitrimers. In the meantime, stress relaxation behavior of vitrimer was evaluated using several fitting models including simple Maxwell model and more complex ones.<sup>4,5</sup> Moreover, numerous monomers and bond exchange reactions (either with or

without catalyst) were introduced to manufacture vitrimer matrices such as transesterification<sup>6,8,18-21,10-17</sup>, disulfide exchange<sup>22,23</sup>, imine bond exchange<sup>24-26</sup>, boronic ester exchange<sup>9</sup>, transamination<sup>27,28</sup>, olefin metathesis<sup>29,30</sup>, and silyl ether bond exchanges<sup>31</sup>.

Notably, epoxy based vitrimer relying on catalysed transesterification are continuously developed due to the versatility of epoxy resin and the reliability of CANs via ester linkages. Many studies attempted to tune the glass transition temperature ( $T_g$ ) of vitrimer formulations. From the literature,  $T_g$  of the synthesized epoxy-acid and epoxy-anhydride vitrimer has been reported in a wide range from -11°C to 187°C.<sup>7,8,32-34,10,14-20</sup> It is well understood that this characteristic strongly depends on the network structure which is directly influenced by a number of epoxide groups on epoxy resin<sup>19</sup> and the chemical structure of hardener.<sup>13,17,20</sup> Following these observations, some groups used off-stoichiometric ratio of starting materials, in particular, carboxyl to epoxy ratio < 1 to alter both thermal and mechanical properties of the vitrimer.<sup>19,33,34</sup> It was demonstrated that excess of epoxy potentially force the formation of rigid non-dynamic crosslinked structure made of ether bond *via* epoxy homopolymerization. Liu and co-workers reported that decreasing anhydride curing agent lead to an increase in Young's modulus of epoxy-anhydride vitrimer although  $T_g$  declined slightly.<sup>19</sup> In epoxy-acid vitrimer, Poutrel et al. and Altuna et al. investigated the systematical increasing in both  $T_g$  and Young's modulus when acid ratio was decreased.<sup>33,34</sup> Additionally, the transition of vitrimer to vitrimer-like material was demonstrated when ratio of carboxyl to epoxy ratio < 0.75 as previously reported and modelled by Torkelson et al., showing full vitrimer characteristic kept up to 60% of exchangeable bonds<sup>35</sup>

Transesterification of epoxy-acid or epoxy-anhydride vitrimer is usually triggered by either organic or metallic catalyst such as Zinc acetate ( $Zn(OAc)_2$ )<sup>6-8,14-19</sup>, Triazobicyclodecene (TBD)<sup>8,20,32,36</sup>, and Triphenylphosphine ( $PPh_3$ )<sup>8</sup>. Nevertheless, it is not only the relatively high cost

of those catalysts,  $\text{Zn}(\text{OAc})_2$  and TBD, which limits the scale-up manufacturing, but also, their low thermal stability leading to the brownish or yellowish of a reprocessed vitrimer.<sup>12,37,38</sup> A potential inexpensive and effective catalysts for transesterification with the antioxidant properties are tin compounds.<sup>39-46</sup> Theoretically, tin exhibits two stable oxidation states including Sn (II) and Sn (IV) which can form complexes with alkyl, oxo, and halide ligands. With their free 5d orbital, tin compounds act as lewis acid in the catalytic transesterification mechanism.<sup>47</sup> It coordinates with electron rich atoms and stimulates the exchange reaction. Additionally, organotin catalyst was reported as an effective stabilizer for rigid PVC.<sup>48-50</sup> Most studies reported the usage of organotin catalyst in transesterification of ester and small alcohol molecules or esterification of fatty acids and polyol.<sup>42,44,51,52</sup> Nevertheless, the potential of using it as catalyst for preparation of the epoxy-acid vitrimer has been confirmed by Liu and coworker.<sup>53</sup> The prepared epoxy-anhydride exhibited flow behavior following an Arrhenius behavior which is one of the characteristic of vitrimers. However, polymerization mechanisms and mechanical performance of the obtained vitrimer remained undefined.

Here, we present an epoxy based vitrimer crosslinked with a cyclic aliphatic dicarboxylic acid catalysed by monobutyltin oxide (Sn). Influence of catalyst concentration as well as off-stoichiometric epoxy:acid ratio were studied for the evolution of active species during synthesis as well as characteristics of the obtained polymer (thermo-mechanical properties and viscoelastic behavior). Additionally, mechanical performances (i.e., tensile, flexural and fracture toughness properties) of epoxy - dicarboxylic acid vitrimer were studied. Finally, healing ability of this system is observed and quantified by single edge notched bending test.

## EXPERIMENTAL SECTION

**Materials.** Commercial epoxy resin used in this study is a diglycidyl ether of bisphenol A (DGEBA) containing reactive diluent (Araldite LY564, epoxy equivalent weight of 168-175 g eq<sup>-1</sup>), purchased from Mouldlife, UK. Cis and trans mixture of 1, 4 cyclohexane dicarboxylic acid (CHDA, molecular weight of 172.18 g mol<sup>-1</sup>) and monobutyltin oxide (Sn, molecular weight of 208.8 g mol<sup>-1</sup>) were supplied by Tokyo Chemical Industry UK Ltd. 1, 2, 4 trichlorobenzene (TCB) was provided by Sigma-Aldrich. The cycloaliphatic amine (Aradur 2954) was used as curing agent for preparing the reference epoxy, supplied by Mouldlife, UK. All chemicals were used as received and their chemical structure are shown in Table 1.

Table 1 Chemical compounds used in this study

Chemical compound	Chemical structure	EEW <sup>a</sup> or MW <sup>b</sup> (g/mol)	Acronym
Diglycidyl ether of bisphenol A with reactive diluent		78-86% 168 – 175 <sup>a</sup> 14-22%	DE
Cis and trans 1,4 cyclohexane dicarboxylic acid		172.18 <sup>b</sup>	CHDA
Monobutyltin oxide		208.8 <sup>b</sup>	Sn
2,2'-dimethyl-4,4'-methylenebis (cyclohexylamine)		238.4 <sup>b</sup>	

<sup>a</sup>epoxy equivalent weight (g eq<sup>-1</sup>), <sup>b</sup>Molecular weight (g mol<sup>-1</sup>)

**Manufacture of epoxy vitrimer.** All vitrimers were prepared through one-pot synthesis. To study the effect of catalyst content, the mixture with molar equivalent (meq) ratio of 1:1 epoxide

group to carboxylate group was prepared and the Sn catalyst content was varied from 0 to 10% meq relative to the epoxide groups. The off-stoichiometric study of epoxy/CHDA vitrimer was carried out with decreasing the meq ratio of CHDA to 1:0.90, 1:0.75, 1:0.60 and 1:0.50, fixing the Sn amount to 5% meq. Table 2 shows all samples name with chemical composition made in this study. Monomers and catalyst were mixed in a beaker using an overhead mixer for 24 hours at 50°C. Then, the mixture was degassed to remove bubbles at 50°C in vacuum oven for an hour. The uncured vitrimer solution was then cast in a metal mould and degassed again at 90°C for 3 hours. Finally, the material was cured at 145°C for 8 hours and post-cured at 160°C for 12 hours.

Table 2 Composition and sample name of vitrimer formulations.

Sample name	Component	
	Epoxy: COOH (molar equivalent ratio, meq)	Sn (%meq to epoxide group)
<b>CHDA100_Sn0</b>	1:1	0
<b>CHDA100_Sn1</b>	1:1	1
<b>CHDA100_Sn5</b>	1:1	5
<b>CHDA100_Sn10</b>	1:1	10
<b>CHDA90_Sn5</b>	1:0.90	5
<b>CHDA75_Sn5</b>	1:0.75	5
<b>CHDA60_Sn5</b>	1:0.60	5
<b>CHDA50_Sn5</b>	1:0.50	5

**IR monitoring of the curing process.** Attenuated total reflection Fourier-transform infrared spectroscopy (ATR-FTIR) was carried out on Bruker INVENIO<sup>®</sup> to analyse the vitrimers and to monitor the polymerization reactions during cure. To monitor the curing reaction, the liquid sample was dropped on an ATR-golden gate accessory set at 145°C. Spectra were collected between the wavenumber of 4000 to 400 cm<sup>-1</sup> for 8 hours. Resolution and number of scans was set at 4 cm<sup>-1</sup> and 8 accumulations.

**Swelling tests.** To confirm the network cross-linking, samples with dimension of  $5 \times 5 \times 5 \text{ mm}^3$  were immersed in TCB at  $150^\circ\text{C}$  until equilibrium (3 days). For soluble fractions, swollen samples were dried in vacuum oven at  $160^\circ\text{C}$  until solvent was fully removed. Swelling ratio and soluble fraction were calculated regarding to equation S1 and S2.

**Dynamic mechanical analysis (DMA), creep test and stress relaxation experiment.** Both thermo-mechanical properties and viscoelastic properties were investigated using a Q800 from TA instrument (USA). For DMA, rectangular samples with dimension of  $10 \times 35 \times 4.5 \text{ mm}^3$  were tested from  $0^\circ\text{C}$  to  $200^\circ\text{C}$  with a heating rate of  $3^\circ\text{C}/\text{min}$  and frequency of 1 Hz using a single cantilever clamp. The glass transition temperature ( $T_g$ ) was indicated from the tan delta peak. Creep tests were also investigated on the same size specimens and same clamp geometry to DMA specimens. The samples were first stabilized above  $T_g$  before being deformed at a constant stress of 0.05 MPa (for 1:1 vitrimer formulations with different Sn content) or 0.1 MPa (for all vitrimers formulations with 5%meq catalyst). Stress relaxation experiments were carried out using shear sandwich geometry with samples cut into squares ( $10 \text{ mm} \times 10 \text{ mm} \times 5 \text{ mm}$ ). The relaxation modulus ( $G$ ) was measured over time with a constant applied strain of 1 %, and values of  $G$  were monitored from  $160^\circ\text{C}$  to  $260^\circ\text{C}$  every  $20^\circ\text{C}$ .

**Mechanical performances.** Tensile tests were performed following ASTM D638 type I dumbbell specimen<sup>54</sup> on an Instron 5956 with crosshead speed of  $5 \text{ mm}\cdot\text{min}^{-1}$  (or strain rate of  $0.00013 \text{ s}^{-1}$ ). Displacements were recorded with an extensometer MTS 634. To obtain standard deviation, five specimens were measured for each formulation.

Flexural tests were conducted according to ASTM D790 with rectangular specimens ( $12.6 \text{ mm} \times 165 \text{ mm} \times 4 \text{ mm}$ ). Three-point bending configuration with a span of 64 mm was set up on an

Instron 5956. Testing was performed at crosshead speed of  $1.7 \text{ mm}\cdot\text{min}^{-1}$  (or strain rate of  $0.00017 \text{ s}^{-1}$ ).

Fracture toughness was measured using single edge notched bending (SENB) according to ASTM D5045.<sup>55</sup> Rectangular specimens of  $18 \text{ mm} \times 85 \text{ mm} \times 5 \text{ mm}$  were V-notched using a milling machine. The razor blade was inserted to create natural crack as shown in Figure S1. Three-point bending configuration was set up on Instron 5956 with a constant displacement of  $0.5 \text{ mm}\cdot\text{min}^{-1}$ . Fracture toughness ( $K_{Ic}$ ) and fracture energy ( $G_{Ic}$ ) were calculated following equations S3 and S4.

**Fractography.** Fracture surface (from SENB samples) testing was observed by scanning electron microscopy (SEM, TESCAN MIRA3) with a 3 nm Au/Pd (80/20) coating.

**Healing experiment.** Fractured samples from SENB tests were healed using hot press at  $200^\circ\text{C}$  (CHDA100\_Sn5, CHDA90\_Sn5 and CHDA75\_Sn5 samples) or  $240^\circ\text{C}$  (CHDA60\_Sn5 and CHDA50\_Sn5 samples) with an applied pressure of 10 bar for 90 min.

## RESULTS AND DISCUSSION

**Synthesis and network structure of epoxy-CHDA vitrimer.** IR spectra of samples before and after curing are presented in Figure 1. The uncured spectrum reveals the main characteristic peaks of both components (epoxy resin and dicarboxylic acid). The epoxide ring of epoxy resin is observed at  $913\text{ cm}^{-1}$  while the complex absorption pattern between  $1100 - 1200\text{ cm}^{-1}$  represents the C-O vibration of the mixture. For CHDA, the carbonyl groups signatures are identified at  $1705\text{ cm}^{-1}$  and  $1735\text{ cm}^{-1}$ .<sup>56</sup> These two wavenumbers are respectively assigned to dimeric and monomeric structure of dicarboxylic acid in the mixture.<sup>56</sup> The broad peak of O-H stretching at  $3200 - 2500\text{ cm}^{-1}$ , overlaying with signal of C-H stretching is characteristic of the OH functional groups from the CHDA compound. FTIR spectrums of raw materials are presented in Figure S2. After curing, the signatures of the epoxide ring and carboxylic acid have completely disappeared, indicating full consumption of reactive groups. The vibration band characteristic of ester bonds at  $1730\text{ cm}^{-1}$  is noticeable in the IR spectrum of the cured sample (Figure 1). The broad peak of hydroxyl groups from ester chains is also observed between  $3200\text{ cm}^{-1} - 3600\text{ cm}^{-1}$ .

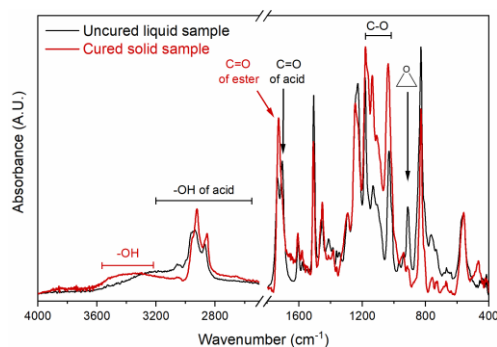
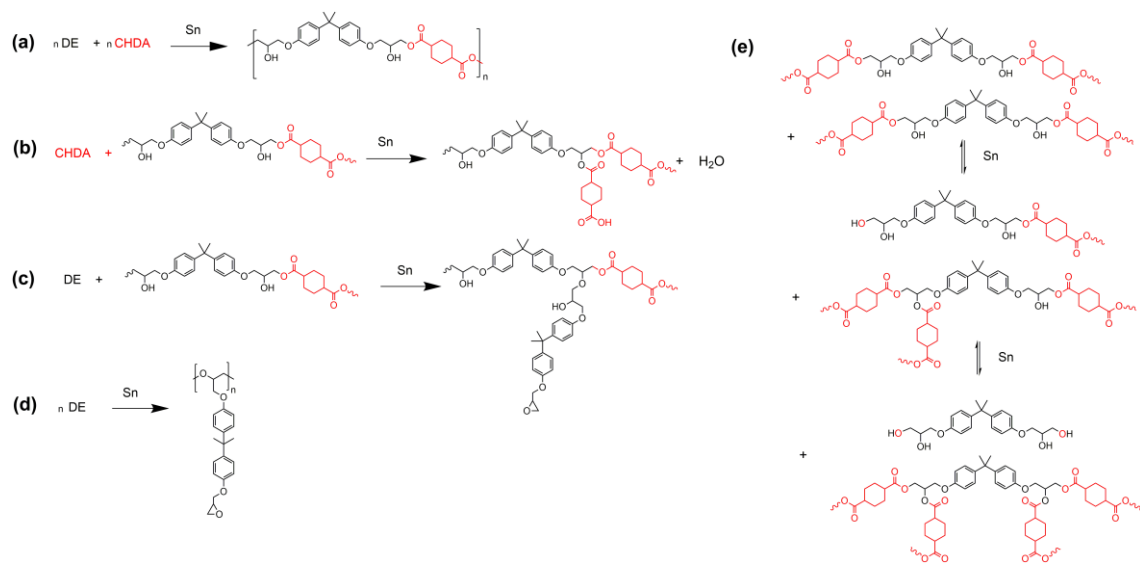


Figure 1 FTIR spectra of CHDA100\_Sn5 before (uncured liquid sample, black curve) and after curing (cured solid sample, red curve).

From these FTIR spectra, the reactions during vitrimer synthesis are proposed in scheme 1. The polyaddition of epoxy resin and dicarboxylic acid is first considered as presented in Scheme 1a.

This reaction is commonly mentioned as the initial reaction of diacid-diepoxy with catalyst.<sup>57-59</sup> It results in the formation of  $\beta$ -hydroxyl ester characteristic of vitrimer prototypes.<sup>6</sup> Thus, the signal of ester bond (COOR) at  $1730\text{ cm}^{-1}$  and hydroxyl group (OH)  $3200\text{ cm}^{-1}$ – $3600\text{ cm}^{-1}$  are found in the spectrum of cured sample. Nonetheless, a single polyaddition reaction leads to the formation of long linear polymeric chains not crosslinked together, not allowing to obtain a gel. A number of side reactions have to be considered to obtain a 3D crosslinked network. The secondary hydroxyl group (OH) obtained from the epoxy-CHDA addition reaction is likely to react via condensation-esterification<sup>59</sup> or etherification<sup>59</sup> (Scheme 1b and 1c). Moreover, epoxy homopolymerization under catalytic ring-opening polymerization (ROP) is also considered when epoxy groups are present in excess under acidic condition as present in Scheme 1d.<sup>60,61</sup> Additionally, transesterification reactions (triggered by the catalyst, Scheme 1e) is also responsible for the formation of network and diglycol unit during polymerization.<sup>34</sup> In order to monitor those reactions, in-situ FTIR is able to reveal the ester formation due to polyaddition and condensation-esterification. However, it would be a challenge to distinguish the etherification because of the complex FTIR band.



Scheme 1 Reactions in vitrimer synthesis:(a) acid-epoxy addition reaction, (b) condensation-esterification of acid and hydroxyl group, (c) ring-opening of epoxide (ROP) via hydroxyl group, (d) catalytic ROP of diepoxy (homopolymerization), (e) transesterification of secondary hydroxyl group and ester linkages.<sup>34,59,61</sup>

**Curing kinetics – IR analysis of catalyst content influence on network formation.** Figure 2 shows the IR spectrums during cure of the CHDA100\_Sn5 sample at 0 min, 30 min and 120 min. To study species evolution over time, the area of four characteristic signatures are labelled in Figure 2. This include the C=O stretching of ester (COOR) at  $1730\text{ cm}^{-1}$ , C=O stretching of diacid (COOH) at  $1705\text{ cm}^{-1}$ , C–O stretching of epoxide ring (Epoxy) at  $913\text{ cm}^{-1}$  and C–O stretching of aliphatic ether (COC) at  $1150\text{--}1120\text{ cm}^{-1}$ ; evaluation of those are described in the supporting information. The C=C stretching signature of aromatic ring at  $1500\text{ cm}^{-1}$  was chosen as an internal reference to calculate the normalized relative peak area. Notation of those signatures are resumed in Table 3.

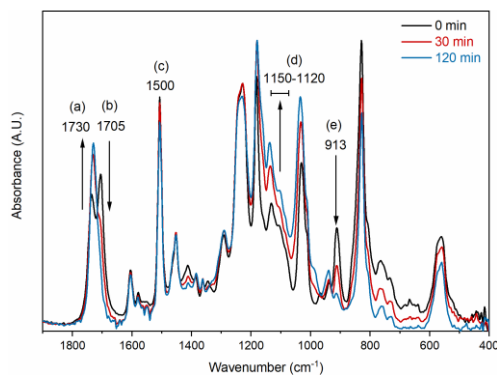


Figure 2 FTIR spectrum of CHDA100\_Sn5 during cure at 145°C after 0 min (black curve), 30 min (red curve), and 120 min (blue curve). (a) C=O stretching of carboxylic acid (COOH), (b) C=O stretching of ester (COOR) (c) C=C stretching of aromatic ring used as an internal reference (d) C–O stretching of alkyl ether (COC), (e) C–O asymmetric stretching of epoxide ring. FTIR spectrum until 480 min is presented in Figure S5.

Table 3 Labels of chemicals moieties investigated.

Species	Wavelength (cm <sup>-1</sup> )	Label
C=O stretching of carboxylic acid	1730	COOH
C=O stretching of ester	1705	COOR
C–O stretching of alkyl ether	1150-1120	COC
C–O asymmetric stretching of epoxide ring	913	Epoxy(ies/ide) (ring)

The effect of catalyst content (0 to 10% meq) on the evolution of those four species are illustrated in Figure 3. As presented in Figure 3a and 3b, the relative signatures of COOH and epoxide groups decrease with time due to the consumption of these species (i.e. via polyaddition). On the other hand, the signatures of COOR and COC arise with the formation of polyester and polyether chains as shown in Figure 3c and d. The addition of organotin catalyst especially at 5% and 10% promotes the reactions mentioned in Scheme 1 as the conversion of all species is accelerated, compared to

the one without the catalyst. At 1% loading, the catalyst does not seem to accelerate significantly the reactions. In principle, it is possible that Lewis acid catalysts, such as monobutyltin oxide, also promotes the formation of ether bond rather than the ester bond when hydroxyl groups are presented.<sup>62</sup> However, the rate of CHDA consumption is faster than the one of epoxides at 5% and 10% catalyst loading (Figure 3a and 3b). For example, at 10% catalyst loading, the epoxide signature takes ~80 min to reach a plateau while it takes only 30 min for the COOH ones. This suggests that the reaction is initially dominated by both epoxy-acid polyaddition and condensation-esterification (Scheme 1a and 1b respectively). Then, the excess of epoxy groups undergoes etherification via hydroxyl group and homopolymerization (Scheme 1c and 1d). At the end of curing, the signal of ester (COOH) is at similar level for any catalyst content, whilst ether bond signature is found to be significantly higher when 10% of catalyst was used. This suggest that 5% of organotin catalyst is not only sufficient to accelerate the reaction in the vitrimer synthesis but also limiting the number of secondary reactions (such as Scheme 1c, consuming free hydroxyl groups) leading to the formation of irreversible ether bonds. Therefore, in order to obtain a vitrimer network with a reasonable amount of free hydroxyl groups, required for the transesterification to happen, the catalyst content was set to 5% for the rest of the study.

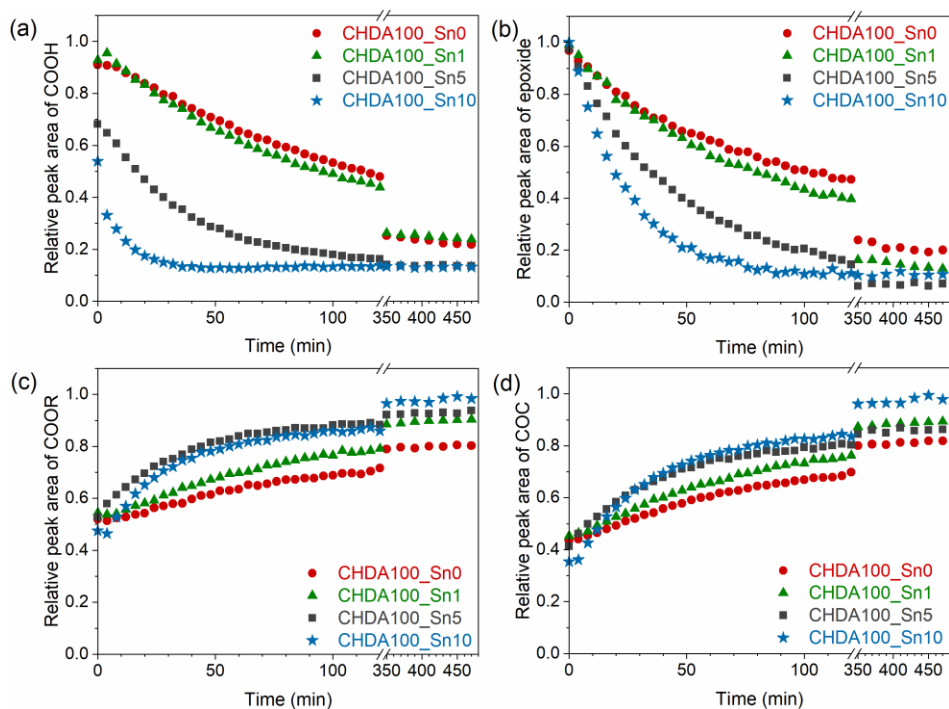


Figure 3 Influence of catalyst content on evolution of species during curing stage (a) C=O stretching of carboxylic acid, COOH, (b) C-O stretching of epoxide ring, (c) C=O stretching of ester, COOR, (d) C–O stretching of alkyl ether, COC.

**Cure kinetics – IR analysis of CHDA content.** Influence of epoxy:CHDA ratio on chemical species evolution are presented in Figure 4. In Figure 4a, COOH species decline with similar rate in all samples, but reach a plateau at different time due to the difference in initial quantity at  $t = 0$  min. It is worth mentioned that once all acid is consumed, a slight increase of acid can be seen due to an artefact of the deconvolution process on the carbonyl signal (C=O) of carboxylic acid and ester as described in ESI. However, it does not interfere the overview trend of acid consumption. Unlike CHDA, the epoxide groups signature of all samples decreases at the same rate during cure as shown in Figure 4b. In term of bond formation, the ester signatures (COOR) of samples with ratio 1:1 and 1:0.9 increase linearly before slowing down toward a plateau. However, that trend changes for samples with high epoxy excess (CHDA75\_Sn5, CHDA60\_Sn5 and CHDA50\_Sn5).

A stepwise increasing of ester species (COOR) was observed in these samples as shown in Figure 4c. For CHDA75\_Sn5, COOR signature increases and reaches a first plateau after 65 minutes. Similarly, plateau is reached at 45 min for CHDA60\_Sn5 and at 25 min for CHDA50\_Sn5. This suggests that the formation of ester linkages was slowed down. It is potentially due to the concurrence with either etherification or homopolymerization (COC signature of aliphatic ether linearly increase when COOR signature reached first plateau, Figure 4d) once most of the acids have been consumed (~90%). It was previously reported that epoxy homopolymerization happens after polyaddition in epoxy-acid vitrimers comprised of long polymer chains<sup>34</sup>. Here our results suggest that for a formulation with cyclic hardener (CHDA) catalyzed by Sn compound, the etherification happens at the same time as polyaddition

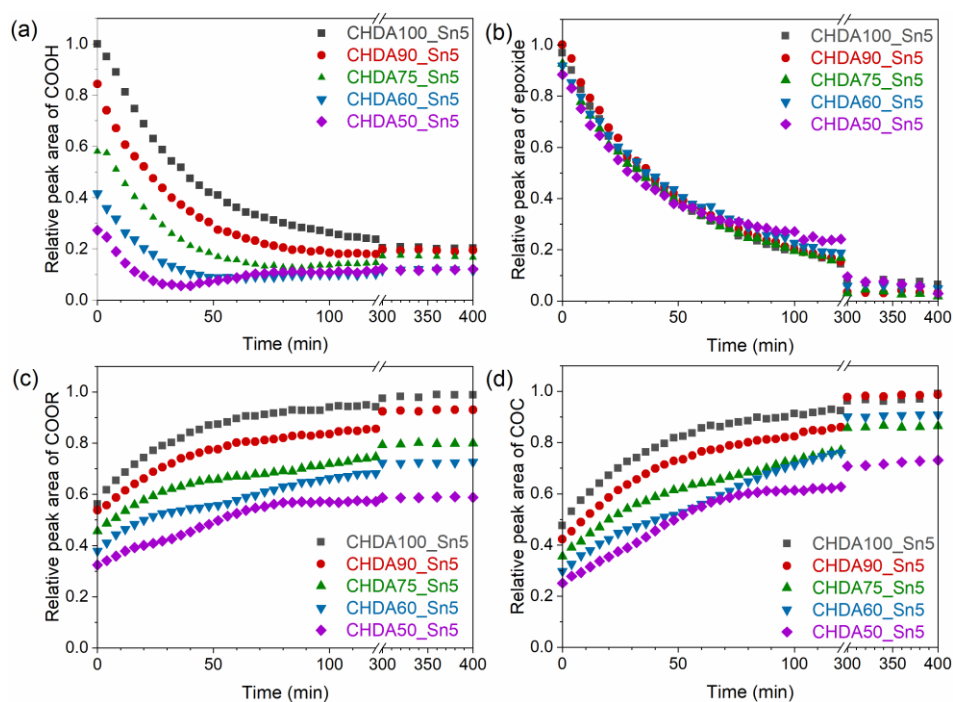


Figure 4 Influence of CHDA content on evolution of species during curing stage (a) C=O stretching of carboxylic acid, COOH, (b) C-O stretching of epoxide ring, (c) C=O stretching of ester, COOR, (d) C-O stretching of alkyl ether, COC.

**Swelling and soluble fraction.** The influence of catalyst content on swelling behavior is presented in Figure 5a. All prepared samples were well swollen with a ratio of ~80-90%, confirming crosslinking of the network. Without monobutyltin oxide, the network structure is able to be formed because dicarboxylic compound function as catalyst<sup>63</sup>, promoting all reactions in Scheme 1 except transesterification. When 1 % tin catalyst was added, kinetic of reaction is similar to the one without catalysts (as discussed in our FTIR results) but transesterification took place during cure of CHDA100\_Sn1. It is potentially resulted in the formation of di-, tri- and tetraglycol (Scheme 1e), leading to a network more crosslinked with exchangeable bonds (ester linkage with pendant hydroxyl functions). Hence, CHDA100\_Sn1 still exhibit a low soluble fraction (9%) but it shows the highest swelling ratio (~90%). At higher catalyst loading (5-10 %), the etherification leads to a tighter crosslinked network, therefore, both the soluble fraction and swelling ratio are decreased (~5% and ~85% respectively.)

The effect of epoxy:CHDA ratio on swelling behavior of vitrimers is presented in Figure 5b. The swelling ratio of vitrimer CHDA100\_Sn5, CHDA90\_Sn5 and CHDA75\_Sn5 are comparable at ~80-90%. It then drops to 58% and 48% for CHDA60\_Sn5 and CHDA50\_Sn5, respectively. This further confirms a higher crosslink density of these off-stoichiometric vitrimer resulting from the presence of ether bonds in these formulations with epoxy excess.

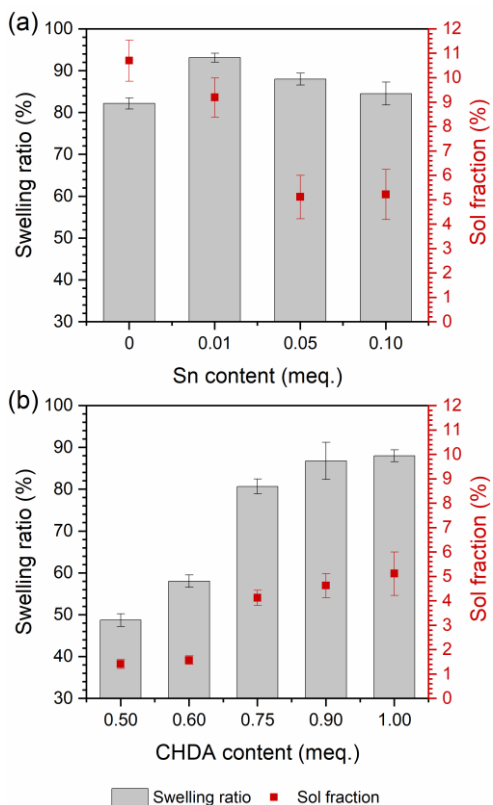


Figure 5 Swelling ratio and sol fraction of epoxy-CHDA vitrimer

**Dynamic mechanical analysis (DMA).** The effect of catalyst content on storage modulus ( $E'$ ) and loss factor ( $\tan \delta$ ) are shown in Figure 6.  $E'$  of all samples, in the glassy state, are very similar until the transition state (Figure 6a). Without catalyst, the first step transition is observed at  $\sim 50^\circ\text{C}$ . It suggests an inhomogeneous network of CHDA100\_Sn0 due to long curing time and low miscibility of the products, not observable through optical microscopy. With catalyst addition, that transition vanishes, suggesting the obtention of a more homogenous network due to a full cure either by esterification or etherification. The onset of  $\alpha$ -transition is shifted to higher temperature when 5% and 10% organotin catalyst was added but values remain close to the one with 1% catalyst loading concurring with soluble fraction results presented earlier (5 and 10% presents lower soluble fraction indicating a higher crosslink density). At the rubbery region, vitrimer with

10% catalyst show lower value of  $E'$  at rubbery region compared to the 5% one, this explained with the help of  $\tan \delta$  analysis. From  $\tan \delta$  data (Figure 6b), the glass transition temperature of samples ( $T_g$ ) were evaluated and are summarized in Table 4.  $T_g$  of all formulations are in the range of 85 - 90°C. At 140°C of  $\tan \delta$  data of CHDA100\_Sn10, mobility of another network type was observed, indicating the heterogeneity in the network. It is possibly due to the microphase separation of product from etherification which is a non-dynamic covalent network. In addition, these separation phases with catalyst pockets playing the role of a plasticizer inside the matrix might explain the drop of  $E'$  in the rubbery region of Sn10 sample compared to the Sn5 one. The catalyst concentration, therefore, do not affect the chemical structure of the polymer but does determine its structure at the microscale (obtention of homogeneous or inhomogeneous polymer). Additionally, this organotin catalyst exhibit a good stability at high temperature up to 200°C. To concisely compare the thermal stability of catalyst, an epoxy vitrimer with triazabicyclodecene (TBD), a well-known organic catalyst in vitrimer synthesis<sup>8,20,36,64</sup>, was manufactured and tested *via* DMA. As shown in Figure S9, the vitrimer using TBD as catalyst turned brown due to the oxidation and decomposition of the catalyst after DMA testing while the vitrimer with Sn just became pale yellow. This suggests that the Sn catalyst is more suitable for vitrimer based on transesterification with high working temperature ( $> 190^\circ\text{C}$ ), especially for their recycling and reprocessing.

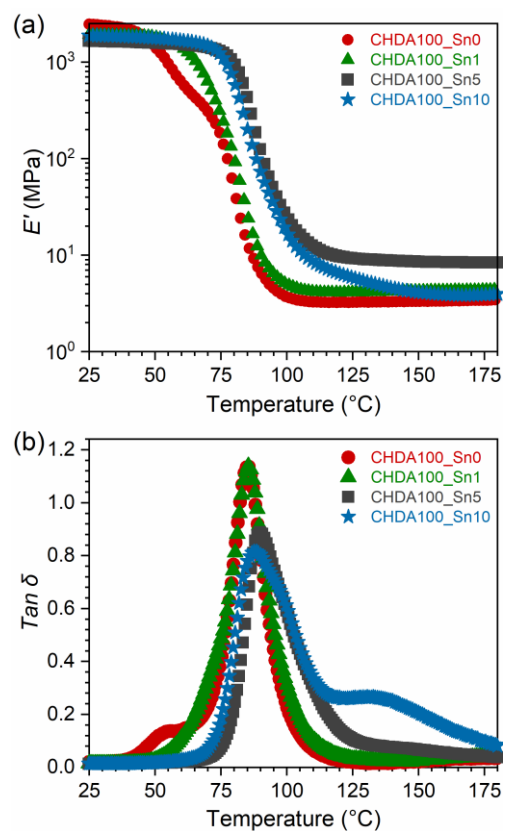


Figure 6 Plot of storage modulus  $E'$  (a) and  $\text{Tan } \delta$  (b) versus temperature for samples with various catalyst loading.

Influence of epoxy:CHDA ratio on both  $E'$  and  $\text{tan } \delta$  is illustrated in Figure 7.  $E'$  at glassy state are slightly varied but they remained stable until the  $\alpha$ -transition. Samples with epoxy:acid ratio 1:60 and 1:0.50 obviously shift the onset of the transition to higher temperature. Additionally,  $E'$  at rubbery plateau of those vitrimers significantly increases compared to the stoichiometric vitrimer as summarized in Table 5.  $E'$  at rubbery state of CHDA60\_Sn5 and CHDA50\_Sn5 is respectively  $\sim 2.7$  and  $\sim 3.7$  times higher than that of CHDA100\_Sn5. This result confirms that both CHDA60\_Sn5 and CHDA50\_Sn5 have a higher crosslink density than CHDA100\_Sn5 due to etherification of epoxides groups with themselves or hydroxyl groups.

$T_g$  of the off stoichiometric vitrimers was obtained from temperature at the peak of  $\tan \delta$  plot in Figure 7b and reported in Table 5.  $T_g$  gradually increase from 90°C to 99°C when CHDA ratio declines from 1.0 to 0.75. By further reduction of acid ratio, there is a remarkable shift on  $T_g$  of the vitrimer with high epoxy excess.  $T_g$  of CHDA60\_Sn5 and CHDA50\_Sn5 were measured at 121°C and 131°C, respectively. The effect of the epoxy excess in off-stoichiometric formulation is further seen when analyzing the damping curves in Figure 7b. For sample CHDA100\_Sn5, the peak is fairly symmetrical. When shifting to lower acid content (90 and 75), the possible microphase of homopolymerized epoxy within the ester network show a progressive apparition of a shoulder on tan delta peak. Moving toward CHDA60\_Sn5 and CHDA50\_Sn5, a clear separation of these board peaks is visible due to the duality of the network rich in ester and ether phases. This observation agrees with the peak observed around 140°C for the case of the high catalyst content (10 %) which heterogeneous network was discussed on Figure 6b. Moreover, peak height of  $\tan \delta$  declines for vitrimer with less CHDA ratio. This further confirms that the high excess of epoxy function leads to their addition onto  $\beta$ -hydroxyl groups, and their homopolymerization as depicted in Scheme 1c and 1d. These two reactions bring a tighter and stiffer crosslink network with lower damping properties that correlates with previous swelling and solubility tests.

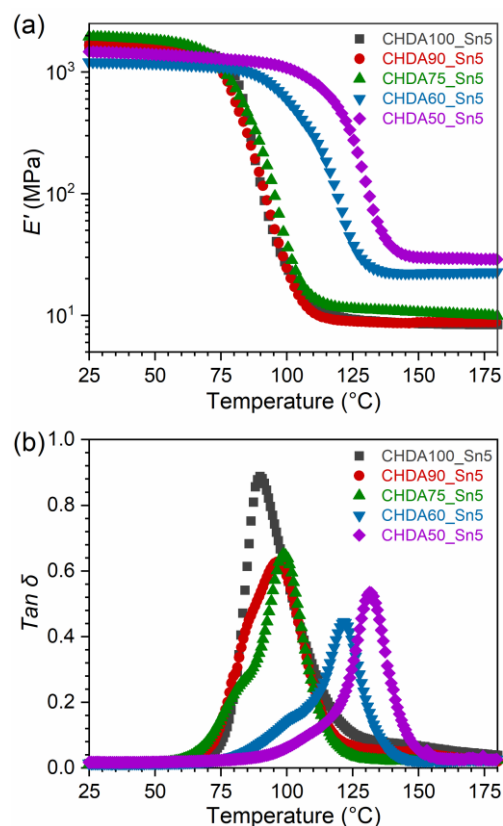


Figure 7 The plot of storage modulus  $E'$  (a) and  $\text{Tan } \delta$  (b) versus temperature for sample with different CHDA content

**Creep and Stress relaxation.** Both creep and stress relaxation of vitrimers were asserted below decomposition temperature ( $T_d$ ) taken at 5% weight loss (TGA, Figure S10). Figure 8a shows creep of samples containing various amount of organotin catalyst at 200 $^{\circ}\text{C}$ . Samples without catalyst and with 1% catalyst loading show a relatively small creep ( $< 0.2\%$ ) compared to the vitrimer containing 5–10% catalyst ( $> 0.8\%$ ). In addition, creep behavior of CHDA100\_Sn5 and CHDA100\_Sn10 show a typical temperature dependence of vitrimers, as presented in Figure S11, suggesting that a sufficient amount of catalyst ( $\geq 5\%$  meq) is necessary to produce the dynamic network.

Figure 8b illustrates the normalized relaxation modulus ( $G_t/G_0$ ) at 200°C over time for samples with different catalyst loading. The non-normalized data also presented in Figure S13. All samples demonstrate relaxation over time. The permanent crosslinked polymer (0% catalyst) can relax partially the stress due to dangling chains and oligomers but not reach full stress relaxation. In this study, although we did not examine CHDA100\_Sn0 until it reaches a plateau, it is clear that the addition of catalyst accelerates the stress relaxation of this network. It is also interesting to note that stretched exponential function give a better fitting with the data from CHDA100\_Sn0, indicating distribution of relaxation rate.<sup>4,65</sup> On the other hand, the generalized Maxwell model with two-phase exponential fits well ( $R^2 = 0.99$ ) the stress relaxation behavior of all prepared vitrimers, suggesting multimode relaxation<sup>64</sup>. The curve fitting and fitting parameter are shown in Figure S14 and S15. From these data, the energy activation ( $E_a$ ) were calculated regarding to Arrhenius's law while the viscoelastic solid-liquid transition temperature ( $T_v$ ) were obtained at temperature corresponding to the relaxation time at  $10^6$  s as described in ESI.

In Figure 8b, the relaxation time ( $\tau^*$ ) of vitrimer concomitantly decreases with higher catalyst loading. At 200°C,  $\tau^*$  of CHDA100\_Sn1, CHDA100\_Sn5 and CHDA100\_Sn10 are observed at 5375 s, 1334 s, and 880 s, respectively. According to the Arrhenius's law, we found that the catalyst content has less influence on  $E_a$  (~90-100 kJ mol<sup>-1</sup>). However, a significant impact on  $T_v$  is observed, which decreases from 110°C to 100°C with higher catalyst content (Figure 8c) as reported by Capelot et al..<sup>16</sup> To summarize, the concentration of catalyst does not influence the energy barrier for exchange reaction but it decrease  $T_v$  of these dynamic polymers.

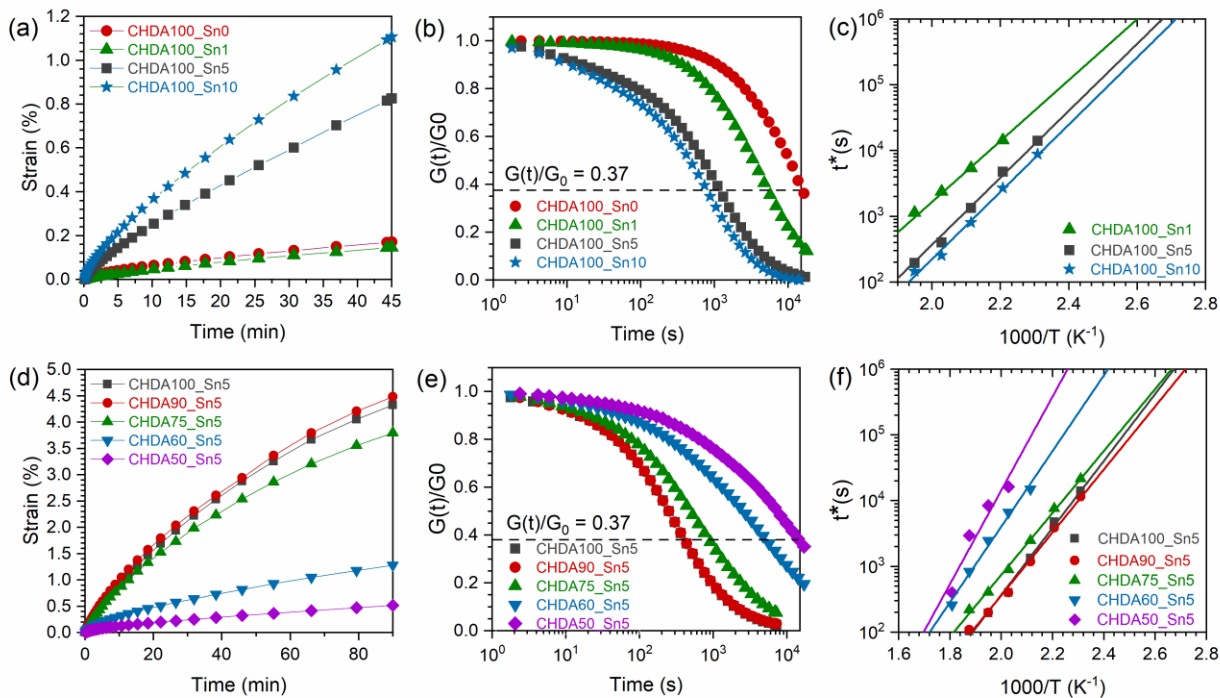


Figure 8 Creep behavior and stress relaxation curves of epoxy-CHDA vitrimers: (a) influence of catalyst content on creep behavior at 200°C with 0.05 MPa applied stress, (b) influence of catalyst loading on the normalized relaxation modulus at 200°C with 1% applied strain, (c) plot of relaxation time in log scale for evaluating  $T_v$  (intersection with top axis) of vitrimers at different catalyst loading, (d) influence of epoxy:CHDA ratio on creep behavior at 220°C with 0.1MPa applied stress, (e) influence of epoxy:CHDA ratio on the normalized relaxation modulus at 220°C with 1% applied strain, (f) plot of relaxation time (log scale) to evaluate  $T_v$  of vitrimers comprised of different ratio.

Table 4 Influence of Sn catalyst content on thermal, dynamic mechanical and viscoelastic properties of epoxy-CHDA vitrimer.

Sample	$T_g$ (°C) <sup>a</sup>	$E'$ (MPa) <sup>b</sup>	$\tau^*$ (s) <sup>c</sup>	$T_v$ (°C) <sup>d</sup>	$E_a$ (kJ mol <sup>-1</sup> ) <sup>e</sup>
CHDA100_Sn0	85.0 ± 2.3	3.4 ± 0.9	-	-	-
CHDA100_Sn1	84.1 ± 1.5	3.1 ± 0.9	5375	111	89
CHDA100_Sn5	90.0 ± 0.4	8.1 ± 1.9	1334	100	98
CHDA100_Sn10	86.5 ± 1.6	6.8 ± 0.3	880	97	99

<sup>a</sup> Glass transition temperature ( $T_g$ ) at  $\tan \sigma$  peak. <sup>b</sup> Storage modulus ( $E'$ ) at rubbery stage ( $T_g+30$  K). <sup>c</sup> Relaxation time ( $\tau^*$ ) when  $G_t/G_0 = 0.37$  at 200°C. <sup>d</sup> Viscoelastic solid-liquid transition temperature ( $T_v$ ) at  $\tau^* = 10^6$  s. <sup>e</sup> Activated energy ( $E_a$ ) from stress relaxation.

Table 5 Influence of CHDA ratio on thermal, dynamic mechanical and viscoelastic properties of epoxy-CHDA vitrimer.

Sample	$T_g$ (°C) <sup>a</sup>	$E'$ (MPa) <sup>b</sup>	$\tau^*$ (s) <sup>c</sup>	$T_v$ (°C) <sup>d</sup>	$E_a$ (kJ mol <sup>-1</sup> ) <sup>e</sup>
CHDA100_Sn5	90.0 ± 0.4	8.1 ± 1.9	401	100	98
CHDA90_Sn5	95.3 ± 1,6	9.0 ± 1.0	400	95	92
CHDA75_Sn5	98.5 ± 1.8	10.9 ± 1.8	890	102	90
CHDA60_Sn5	121.3 ± 0.3	21.8 ± 0.5	5335	140	110
CHDA50_Sn5	131.1 ± 0.8	29.8 ± 0.3	16275	170	136

<sup>a</sup> Glass transition temperature ( $T_g$ ) at  $\tan \sigma$  peak. <sup>b</sup> Storage modulus ( $E'$ ) at rubbery stage ( $T_g+30$  K). <sup>c</sup> Relaxation time ( $\tau^*$ ) when  $G_t/G_0 = 0.37$  at 220°C. <sup>d</sup> Viscoelastic solid-liquid transition temperature ( $T_v$ ) at  $\tau^* = 10^6$  s. <sup>e</sup> Activated energy ( $E_a$ ) from stress relaxation.

Influence of epoxy:CHDA ratio on creep and stress relaxation is shown in Figure 8d–f. In Figure 8d, CHDA100\_Sn5 and CHDA90\_Sn5 show similar creep behavior with maximum strain of ~4.5% strain at 220°C. The creep behavior tends to be inhibited with lower CHDA ratio especially for CHDA60Sn5 and CHDA50\_Sn5 (up to 1% and 0.5% creep respectively), a result already observed several times in the vitrimer literature, where the implementation of unexchangeable

bonds improve creep resistance.<sup>34,35</sup> Figure 8e shows the stress relaxation behavior of stoichiometric and off-stoichiometric vitrimer at 220°C. The vitrimers comprised of 1:1 to 1:0.75 epoxy:acid ratio revealed similar relaxation behavior. For system with high epoxy excess, CHDA60\_Sn5 and CHDA50\_Sn5, the relaxation of modulus is delayed. In Figure 8e,  $\tau^*$  of CHDA50\_Sn5 is 16,275 s which is ~40 times higher than CHDA90Sn5 and CHDA100Sn5 ( $\tau^*$  ~400 s and ~401 s, respectively). These viscoelastic behaviors are in agreement with the theoretical study of off-stoichiometric vitrimer.<sup>9</sup> We also found that generalized Maxwell model with 3-phase exponential show a better fitting curve with the experiment data of CHDA60\_Sn5 and CHDA50\_Sn5 (Figure S16), suggesting more complex relaxation behaviors in these crosslinked structures (i.e. combination of relaxations by Rouse reptation, transesterification and other relaxation modes).<sup>66,67</sup> Thus,  $E_a$  of vitrimer with high excess epoxy (CHDA60\_Sn5 and CHDA50\_Sn5) would be referred to overall energies for both exchange reaction and relaxation of macroscopic structure.

Table 5 summarizes  $T_v$  and  $E_a$  of the off-stoichiometric vitrimers from plots and calculations. Both  $E_a$  and  $T_v$  are significantly risen by reducing the amount of diacid ratio to 0.60 and 0.50.  $E_a$  of CHDA50\_Sn5 increases to 136 kJ mol<sup>-1</sup> while  $T_v$  shifts to 170°C. From recent literatures,  $E_a$  of vitrimers based on transesterification are evaluated in the range of 90–130 kJ mol<sup>-1</sup>.<sup>6,8,11,13,14,17</sup> Type of catalyst and network structure are found as the main parameters on this energy activation. For CHDA60\_Sn5 and CHDA50\_Sn5, the epoxy groups in excess promote the etherification, which becomes dominant in the branching to obtain a network. These non-dynamic ether linkages may form microphases in the crosslinked structure, obstructing the movement of active bonds for transesterification as indicated by additional relaxation modes seen from the model fitting.

Therefore, the overall energy for activating the relaxation of these samples, CHDA60\_Sn5 and CHDA50\_Sn5, is increased leading to higher values of both measured  $E_a$  and  $T_v$ .

**Mechanical performance of the off-stoichiometric epoxy/CHDA vitrimer.** Typical stress-strain curves and tensile properties of vitrimer samples are shown in Figure 9 (a) Typical stress-strain  $\sigma$ - $\gamma$  curve and (b) Tensile properties including tensile strength at yield  $\sigma$ , tensile strain at yield  $\gamma$  and Young's modulus E of vitrimer containing various epoxy:CHDA ratio. Figure 9. Compared to the stress-strain curve of the conventional brittle epoxy-amine, epoxy/CHDA vitrimers exhibit a ductile behavior (yielding observed in Figure 9a). This behavior is likely induced by the presence of di, tri-tetraol produced via transesterification equilibrium, giving a network with higher dangling chains than in epoxy-amine formulation. From the plot in Figure 9b, tensile strength of all vitrimer are comparable (~60–64 MPa). However, Young's modulus of CHDA60\_Sn5 and CHDA50\_Sn5 are slightly lower than others as summarized in Table 6. Additionally, elongation at yield gradually increases with decreasing diacid content, suggesting that the ductibility is more pronounced in excess epoxy samples. This result goes in the opposite direction that our previous study with sebacic acid as hardener.<sup>34</sup> In the previous case, the sebacic acid acted more like a “soft crosslinker”, and homopolymerization led to aromatic compound being linked together more closely which resulted in higher E and lower elongation. In the case of the CHDA hardener, as aliphatic cyclic compound with absence of unsaturated chains, the decrease of its content leads to aromatic moieties in the polymer to be less closely linked which results in lower Young's modulus and higher elongation. In other word, the sebacic acid compound of vitrimer formulation can be considered as flexible spacer while CHDA acts as a rigid crosslinker.

Flexural properties were also investigated and summarized in Table 6. Flexural strength of all vitrimers are found to be in the same range of ~100 MPa. The flexural modulus slightly decreases with excess of epoxy (*i.e.* decrease of CHDA content) while %strain at maximum load gradually increases (especially for CHDA60\_Sn5 and CHDA50\_Sn5).

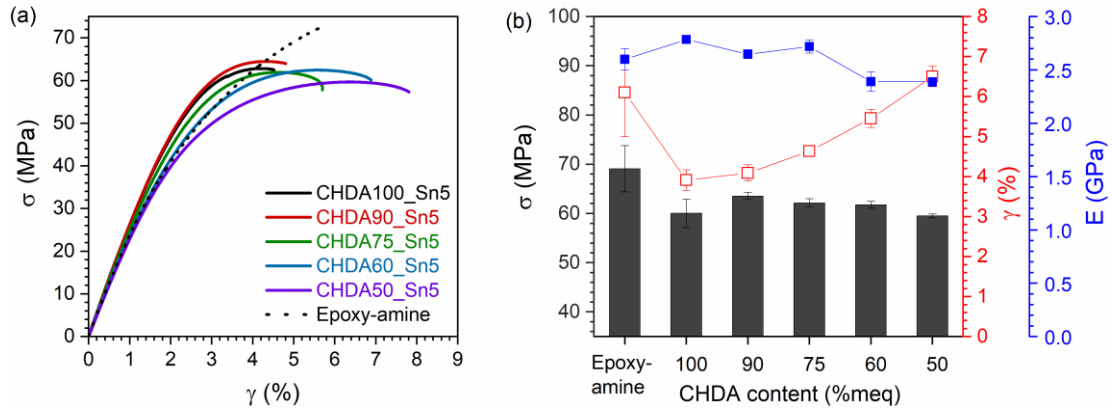


Figure 9 (a) Typical stress-strain  $\sigma$ - $\gamma$  curve and (b) Tensile properties including tensile strength at yield  $\sigma$ , tensile strain at yield  $\gamma$  and Young's modulus  $E$  of vitrimer containing various epoxy:CHDA ratio.

Table 6 Tensile properties (tensile strength at yield  $\sigma_y$ , tensile strain at yield  $\gamma_y$  and Young's modulus  $E_y$ ), Flexural properties and fracture properties (fracture toughness  $K_{Ic}$  and fracture energy  $G_{Ic}$ ) of the off-stoichiometric vitrimer.

Sample	$\sigma_y$ (MPa)	$\gamma_y$ (%)	$E_y$ (GPa)	$\sigma_f$ (MPa)	$\gamma_f$ (%)	$E_f$ (GPa)	$K_{Ic}$ (MPa m <sup>1/2</sup> )
CHDA100_Sn5	60.0 ± 2.9	3.9 ± 0.3	2.8 ± 0.0	104.1 ± 4.3	5.5 ± 0.4	2.7 ± 0.2	0.93 ± 0.04
CHDA90_Sn5	63.5 ± 0.7	4.0 ± 0.2	2.6 ± 0.0	103.6 ± 1.2	5.6 ± 0.2	2.8 ± 0.0	0.93 ± 0.10
CHDA75_Sn5	62.1 ± 0.9	4.6 ± 0.1	2.7 ± 0.1	98.5 ± 1.3	6.3 ± 0.1	2.5 ± 0.1	0.96 ± 0.04
CHDA60_Sn5	61.8 ± 0.7	5.4 ± 0.2	2.4 ± 0.1	100.3 ± 1.3	6.7 ± 0.2	2.5 ± 0.1	1.39 ± 0.08
CHDA50_Sn5	59.5 ± 0.4	6.5 ± 0.3	2.4 ± 0.0	103.9 ± 2.9	7.4 ± 0.2	2.3 ± 0.1	1.59 ± 0.06

Plane-strain fracture toughness ( $K_{Ic}$ ) and fracture energy ( $G_{Ic}$ ) of epoxy-diacid vitrimer was determined and shown in Figure 10. The stoichiometric vitrimer of 1:1 epoxy:acid ratio provide a higher fracture toughness properties than reference epoxy. Some off-stoichiometric vitrimer including CHDA90\_Sn5 and CHDA75\_Sn5 exhibit similar properties to CHDA100\_Sn5 with  $K_{Ic}$   $\sim$ 0.93–0.95 MPa m<sup>1/2</sup>. Drastical improvement of  $K_{Ic}$  and  $G_{Ic}$  is observed in CHDA60\_Sn5 and CHDA50\_Sn5. Among those prepared vitrimer, CHDA50\_Sn5 provide the maximum  $K_{Ic}$  ( $\sim$ 1.59  $\pm$  0.1MPa m<sup>1/2</sup>) which represents 71% improvement compared to CHDA100\_Sn5 or 106 % enhancement compared to epoxy-amine thermoset. From these results a transition from stiff vitrimer to ductile material is observed when epoxy-CHDA vitrimer have  $\geq$  40% excess epoxy ratio. To understand this behavior, SEM analysis of samples was performed to observed their microstructures.

SEM micrographs (Figure 11) illustrates fracture surfaces from the single edge notched bending (SENB) experiment. The sharp plane crack propagation and crack branching was clearly found for 1:1 to 1:0.75 vitrimers (Figure 11a-1, 11b-1 and 11c-1, respectively), similar to the fracture surface of conventional epoxy-amine thermoset (Figure S19). Nevertheless, CHDA60\_Sn5 and CHDA50\_Sn5 clearly exhibit a rougher fracture surface as presented in Figure 11e-1 and 11f-1, respectively. At high magnification (Figure 11e-2 and 11f-2), SEM images reveal coarse and ditches surfaces. This suggests the presence of strain localization during crack propagation for both samples which improved the fracture toughness of these materials. In general, mechanical behavior of polymer is dominated by both extrinsic and intrinsic parameter.<sup>68</sup> In this study, testing conditions such as temperature, speed rate and dimensions, were kept constant so the molecular structure of polymer is responsible for the difference in mechanical results. As demonstrated from DMA, swelling and stress relaxation experiment, the network structure of samples with high

excess epoxy (CHDA60\_Sn5 and CHDA50\_Sn5) are distinguished from the others (CHDA100\_Sn5, CHDA90\_Sn5 and CHHDA75\_Sn5) due to the high ether bonds content. Non-exchangeable bonds of ether linkages potentially form a dense and rigid phase made of non-dynamic crosslinked due to the reaction in Scheme 1c (etherification) and 1d (homopolymerization of epoxy). On the other hand, the dynamic network of ester bond is generated via Scheme 1a (epoxy-acid addition), Scheme 1b (condensation-esterification) and Scheme 1e (transesterification). This part of the network comprised more dangling chain and oligomers due to transesterification giving a softer phase with better damping properties (as seen in DMA results). Therefore, the heterogeneity of network potentially exists in formulations far from the 1:1 stoichiometry such as CHDA60\_Sn5 and CHDA50\_Sn5. This heterogeneity might be slightly detrimental for the network relaxation; however, it is beneficial for the improvement of  $K_{Ic}$  due to the localized area of high molecular mobility at interphase.

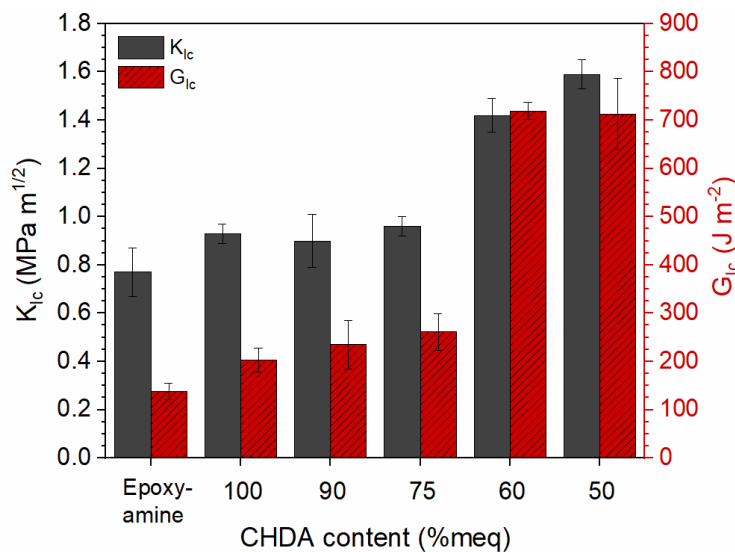


Figure 10 The effect of epoxy:CHDA ratio on fracture toughness  $K_{Ic}$  and fracture energy,  $G_{Ic}$ .

**Self-healing ability.** To investigate the healing ability of vitrimers samples above  $T_v$ , the fractured samples from SENB were compressed via hot press. All healed specimens have been re-

notched and pre-crack in the same manner as the pristine specimens. Figure 12 shows that the fractures of both stoichiometric, CHDA100\_Sn5, and off-stoichiometric, CHDA50\_Sn5, are fully healed after compression. Notably, the V-notch also get smaller, confirming the flow ability of vitrimer above  $T_v$ , making the polymer passing from a viscoelastic solid to a viscoelastic liquid. Fracture toughness of healed vitrimer was also investigated as shown in Figure 13. It is worth noted that all healed specimens have been re-notched and pre-crack same as the pristine specimens. A drop in  $K_{Ic}$  value of less than 10% is observed compared to the pristine sample, indicating good healing for both stoichiometric and off-stoichiometric vitrimers. Fractured surface of healed vitrimers shows similar features to that of pristine vitrimer, especially for 1:1 to 1:0.75 epoxy:acyl vitrimers (see Figure S22). For CHDA60\_Sn5 and CHDA50\_Sn5, the coarse and ditches surfaces are still observed but they are less extensive compared to the neat one.

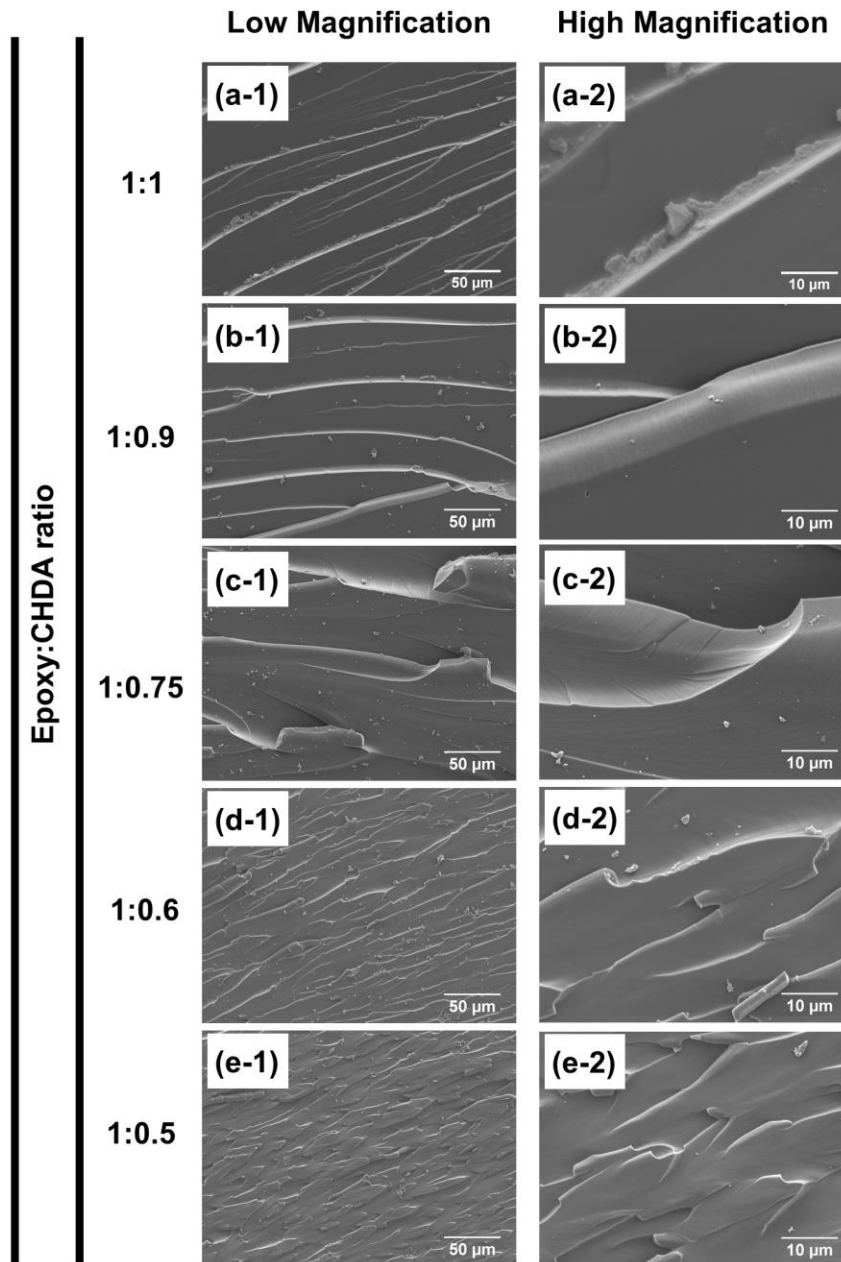


Figure 11 SEM images of fracture surface after SENB testing. (a) CHDA100\_Sn5 (b) CHDA90\_Sn5 (c) CHDA75\_Sn5 (d) CHDA60\_Sn5 and (e) CHDA50\_Sn5 (Crack propagation: left to right).

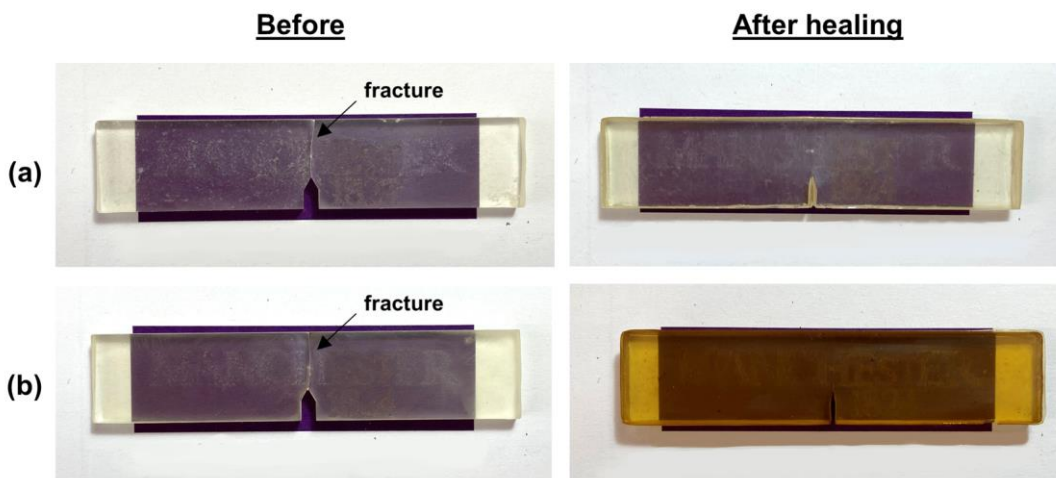


Figure 12 Vitrimer before and after healing using hot compression (a) C100\_Sn5 healed at 200°C for 90 min (b) CHDA50\_Sn5 healed at 240°C for 90 min.

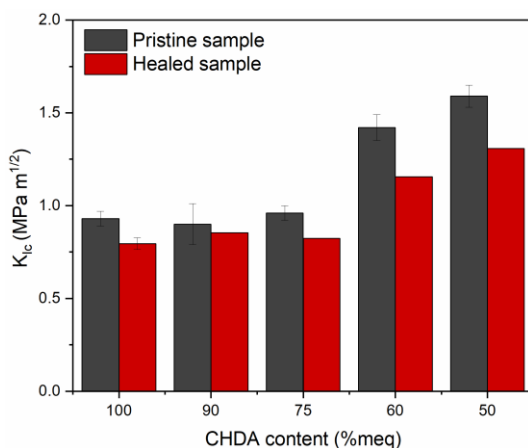


Figure 13 Fracture toughness of pristine and healed vitrimers

## CONCLUSION

In this study, epoxy/CHDA vitrimers were successfully prepared using organotin as a catalyst. The monobutyltin oxide play a role in network formation via the combination of several reactions: epoxy-acid addition, condensation-esterification, etherification, epoxy homopolymerization and transesterification. We found that a sufficient amount of catalyst ( $\geq 5$  mol%) is required to obtain

vitriemer networks able to flow and relax stress, at 1% loading, the polymerization and properties is close to that of a classical thermoset. However, increasing the catalyst content to 10% leads to a vitriemer network with inhomogeneity, therefore it was found that 5% of Sn catalyst was the right amount to produce high  $T_g$  vitrimers. As the major network structure is not affected by the loading of organotin catalyst, the energy barrier of chain exchange reaction ( $E_a$ ) is independent from this loading (5 %meq and 10 %meq) but do affect the freezing topology temperature or  $T_v$ . On the other hand, the vitriemer obtained from high epoxy excess with 5 %meq catalyst exhibit different network structures with higher crosslink density, especially for vitrimers with 1:60 to 1:0.50 epoxy:acid ratio. All  $T_g$ ,  $E_a$  and  $T_v$  are shifted to higher values due to the network intrication with non-exchangeable polyether bonds. This proves that the molecular structure strongly dominates the dynamic behavior of vitriemer (such as  $E_a$ ), while  $T_v$  is controlled by both network structure and the catalyst content. Both stoichiometric and off-stoichiometric vitriemer exhibit excellent tensile properties which is comparable to the epoxy reference. A transition from brittle to ductile fracture is observed when the acid ratio decreases to 0.60. This is attributed to the diminution of rigid crosslinker units (CHDA) within the network leading to aromatic compound being on average less close to each other on the polymer backbone. Among the obtained vitriemer, CHDA60\_Sn5 and CHDA50\_Sn5 exhibit a remarkable fracture toughness improvement (up to 71% compared to the CHDA100\_Sn5) due to the potential strain localization of the inhomogeneous network. These mechanical results combined with relaxation characterizations show that vitriemer can be designed to improve ductility and toughness of epoxy compounds while keeping the vitriemer ability to flow and be healed: both stoichiometric and off-stoichiometric vitriemer are successfully healed under high temperature and pressure. Despite a slight decrease in fracture toughness, the healed samples still exhibited good properties compared with the pristine sample. The ability to keep self-healing

ability, increase creep resistance, and improve toughness of these high  $T_g$  epoxy vitrimer formulations has a strong appeal for application such as composite for aerospace or other structural applications requiring high performance polymers.

## **ASSOCIATED CONTENT**

### **Supporting information**

The supporting information is available free of charge at

Calculation of swelling ratio and %soluble fraction, Calculation of fracture toughness ( $K_{Ic}$ ) and fracture energy ( $G_{Ic}$ ), Fracture toughness specimen, supplementary information for FTIR analysis including experimental procedure, spectra analysis method, spectra of raw materials, spectra of CHDA100\_Sn5 at all reaction time, table of FTIR frequency band, deconvolution area and evolution of species upon reaction time in log scale, comparison of catalyst oxidation in CHDA100 sample, Thermal stability of all samples, supplementary data of creep experiment for all samples, supplementary data of stress relaxation experiment for all samples, fracture surface of epoxy-amine, supplementary information for self-healing experiment (PDF)

## **AUTHOR INFORMATION**

### **Corresponding Author**

Matthieu Gresil – i-composites lab, Department of Material Science and Engineering, Department of Mechanical and Aerospace Engineering, 20 Research Way, Clayton, VIC 3800, Australia.

Email: [matthieu.gresil@monash.edu](mailto:matthieu.gresil@monash.edu)

### **Authors**

Kanokporn Tangthana-umrung – Department of Materials, University of Manchester, UK. Email:

[Kanokporn.tangthana-umrung@postgrad.manchester.ac.uk](mailto:Kanokporn.tangthana-umrung@postgrad.manchester.ac.uk)

Quentin-Arthur Poutrel - Molecular, Macromolecular Chemistry, and Materials, ESPCI Paris, PSL University, CNRS, 10 rue Vauquelin, 75005 Paris, France Email: [quentin-arthur.poutrel@espci.fr](mailto:quentin-arthur.poutrel@espci.fr)

## **ACKNOWLEDGMENT**

We would like to thank Royal Thai government scholarship for financial support. Q-A. P. acknowledges financial support from the European Union's Horizon 2020 research and innovation program under grant agreement No. 828818. The authors would also like to acknowledge François Tournilhac from ESPCI-Paris PSL for his suggestion to use CHDA as chemical to develop vitrimer materials with high glass transition temperature.

## References

- (1) Parameswaranpillai, J.; Hameed, N.; Woo, E. M. *Handbook of Epoxy Blends*; 2017.
- (2) Pascault, J.-P.; Williams, R. J. J. General Concepts about Epoxy Polymers. In *Epoxy Polymers: New Materials and Innovations*; 2010; pp 1–12.
- (3) Carolan, D.; Ivankovic, A.; Kinloch, A. J.; Sprenger, S.; Taylor, A. C. Toughening of Epoxy-Based Hybrid Nanocomposites. *Polym. (United Kingdom)* **2016**, *97*, 179–190.
- (4) Self, J. L.; Dolinski, N. D.; Zayas, M. S.; Read De Alaniz, J.; Bates, C. M. Brønsted-Acid-Catalyzed Exchange in Polyester Dynamic Covalent Networks. *ACS Macro Lett.* **2018**, *7* (7), 817–821.
- (5) Jourdain, A.; Asbai, R.; Anaya, O.; Chehimi, M. M.; Drockenmuller, E.; Montarnal, D. Rheological Properties of Covalent Adaptable Networks with 1,2,3-Triazolium Cross-Links: The Missing Link between Vitrimers and Dissociative Networks. *ACS Appl. Mater. Interfaces* **2020**, *53* (6), 1884–1900.
- (6) Montarnal, D.; Capelot, M.; Tournilhac, F.; Leibler, L. Silica-like Malleable Materials from Permanent Organic Networks. *Science (80-. )*. **2011**, *334* (6058), 965–968.
- (7) Legrand, A.; Soulié-Ziakovic, C. Silica-Epoxy Vitrimer Nanocomposites. *Macromolecules* **2016**, *49* (16), 5893–5902.
- (8) Capelot, M.; Unterlass, M. M.; Tournilhac, F.; Leibler, L. Catalytic Control of the Vitrimer Glass Transition. *ACS Macro Lett.* **2012**, *1* (7), 789–792.
- (9) Meng, F.; Saed, M. O.; Terentjev, E. M. Elasticity and Relaxation in Full and Partial Vitrimer Networks. *Macromolecules* **2019**, *52* (19), 7423–7429.
- (10) Altuna, F. I.; Hoppe, C. E.; Williams, R. J. J. Epoxy Vitrimers: The Effect of Transesterification Reactions on the Network Structure. *Polymers (Basel)*. **2018**, *10* (1).
- (11) Altuna, F. I.; Hoppe, C. E.; Williams, R. J. J. Epoxy Vitrimers with a Covalently Bonded Tertiary Amine as Catalyst of the Transesterification Reaction. *Eur. Polym. J.* **2019**, *113*, 297–304.
- (12) Liu, T.; Zhang, S.; Hao, C.; Verdi, C.; Liu, W.; Liu, H.; Zhang, J. Glycerol Induced Catalyst-Free Curing of Epoxy and Vitrimer Preparation. *Macromol. Rapid Commun.* **2019**, *40* (7).
- (13) Hayashi, M.; Yano, R.; Takasu, A. Synthesis of Amorphous Low: Tg Polyesters with Multiple COOH Side Groups and Their Utilization for Elastomeric Vitrimers Based on Post-Polymerization Cross-Linking. *Polym. Chem.* **2019**, *10* (16), 2047–2056.
- (14) Niu, X.; Wang, F.; Li, X.; Zhang, R.; Wu, Q.; Sun, P. Using Zn 2+ Ionomer to Catalyze Transesterification Reaction in Epoxy Vitrimer. *Ind. Eng. Chem. Res.* **2019**.
- (15) Li, H.; Zhang, B.; Yu, K.; Yuan, C.; Zhou, C.; Dunn, M. L.; Qi, H. J.; Shi, Q.; Wei, Q. H.; Liu, J.; et al. Influence of Treating Parameters on Thermomechanical Properties of Recycled

- Epoxy-Acid Vitrimers. *Soft Matter* **2020**, *16* (6), 1668–1677.
- (16) Capelot, M.; Montarnal, D.; Tournilhac, F.; Leibler, L. Metal-Catalyzed Transesterification for Healing and Assembling of Thermosets. *J. Am. Chem. Soc.* **2012**, *134* (18), 7664–7667.
  - (17) Snijkers, F.; Pasquino, R.; Maffezzoli, A. Curing and Viscoelasticity of Vitrimers. *Soft Matter* **2017**, *13* (1), 258–268.
  - (18) Han, J.; Liu, T.; Hao, C.; Zhang, S.; Guo, B.; Zhang, J. A Catalyst-Free Epoxy Vitrimer System Based on Multifunctional Hyperbranched Polymer. *Macromolecules* **2018**, *51* (17), 6789–6799.
  - (19) Liu, T.; Hao, C.; Zhang, S.; Yang, X.; Wang, L.; Han, J.; Li, Y.; Xin, J.; Zhang, J. A Self-Healable High Glass Transition Temperature Bioepoxy Material Based on Vitrimer Chemistry. *Macromolecules* **2018**, *51* (15), 5577–5585.
  - (20) Chen, J. H.; An, X. P.; Li, Y. D.; Wang, M.; Zeng, J. B. Reprocessible Epoxy Networks with Tunable Physical Properties: Synthesis, Stress Relaxation and Recyclability. *Chinese J. Polym. Sci. (English Ed.)* **2018**, *36* (5), 641–648.
  - (21) Han, H.; Xu, X. Poly(Methyl Methacrylate)–Epoxy Vitrimer Composites. *J. Appl. Polym. Sci.* **2018**, *135* (22), 1–5.
  - (22) Ruiz De Luzuriaga, A.; Martin, R.; Markaide, N.; Rekondo, A.; Cabañero, G.; Rodríguez, J.; Odriozola, I. Epoxy Resin with Exchangeable Disulfide Crosslinks to Obtain Reprocessable, Repairable and Recyclable Fiber-Reinforced Thermoset Composites. *Mater. Horizons* **2016**, *3* (3), 241–247.
  - (23) Liu, J.; Liu, Y.; Wang, Y.; Zhu, J.; Yu, J.; Hu, Z. Disulfide Bonds and Metal-Ligand Co-Crosslinked Network with Improved Mechanical and Self-Healing Properties. *Mater. Today Commun.* **2017**, *13* (November), 282–289.
  - (24) Dhers, S.; Vantomme, G.; Avérous, L. A Fully Bio-Based Polyimine Vitrimer Derived from Fructose. *Green Chem.* **2019**, *21* (7), 1596–1601.
  - (25) Yu, Q.; Peng, X.; Wang, Y.; Geng, H.; Xu, A.; Zhang, X.; Xu, W.; Ye, D. Vanillin-Based Degradable Epoxy Vitrimers: Reprocessability and Mechanical Properties Study. *Eur. Polym. J.* **2019**, *117*, 55–63.
  - (26) Liu, H.; Zhang, H.; Wang, H.; Huang, X.; Huang, G.; Wu, J. Weldable, Malleable and Programmable Epoxy Vitrimers with High Mechanical Properties and Water Insensitivity. *Chem. Eng. J.* **2019**, *368*, 61–70.
  - (27) Stukenbroeker, T.; Wang, W.; Winne, J. M.; Du Prez, F. E.; Nicolaÿ, R.; Leibler, L. Polydimethylsiloxane Quenchable Vitrimers. *Polym. Chem.* **2017**, *8* (43), 6590–6593.
  - (28) Denissen, W.; Winne, J. M.; Du Prez, F. E. Vitrimers: Permanent Organic Networks with Glass-like Fluidity. *Chem. Sci.* **2016**, *7* (1), 30–38.
  - (29) Röttger, M.; Domenech, T.; van der Weegen, R.; Breuillac, A.; Nicolaÿ, R.; Leibler, L.

- High-Performance Vitrimers from Commodity Thermoplastics through Dioxaborolane Metathesis. *Science* (80-. ). **2017**, 356 (6333), 62.
- (30) Lu, Y. X.; Tournilhac, F.; Leibler, L.; Guan, Z. Making Insoluble Polymer Networks Malleable via Olefin Metathesis. *J. Am. Chem. Soc.* **2012**, 134 (20), 8424–8427.
- (31) Wu, S.; Yang, Z.; Fang, S.; Tang, Z.; Liu, F.; Guo, B. Malleable Organic/Inorganic Thermosetting Hybrids Enabled by Exchangeable Silyl Ether Interfaces. *J. Mater. Chem. A* **2019**, 7 (4), 1459–1467.
- (32) Yang, Y.; Zhang, S.; Zhang, X.; Gao, L.; Wei, Y.; Ji, Y. Detecting Topology Freezing Transition Temperature of Vitrimers by AIE Luminogens. *Nat. Commun.* **2019**, 10 (1), 1–8.
- (33) Altuna, F. I.; Hoppe, C. E.; Williams, R. J. J. Shape Memory Epoxy Vitrimers Based on DGEBA Crosslinked with Dicarboxylic Acids and Their Blends with Citric Acid. *RSC Adv.* **2016**, 6 (91), 88647–88655.
- (34) Poutrel, Q. A.; Blaker, J. J.; Soutis, C.; Tournilhac, F.; Gresil, M. Dicarboxylic Acid-Epoxy Vitrimers: Influence of the off-Stoichiometric Acid Content on Cure Reactions and Thermo-Mechanical Properties. *Polym. Chem.* **2020**, 11 (33), 5327–5338.
- (35) Li, L.; Chen, X.; Jin, K.; Torkelson, J. M. Vitrimers Designed Both To Strongly Suppress Creep and To Recover Original Cross-Link Density after Reprocessing: Quantitative Theory and Experiments. *Macromolecules* **2018**, 51 (15), 5537–5546.
- (36) He, C.; Shi, S.; Wu, X.; Russell, T. P.; Wang, D. Atomic Force Microscopy Nanomechanical Mapping Visualizes Interfacial Broadening between Networks Due to Chemical Exchange Reactions. *J. Am. Chem. Soc.* **2018**, 140 (22), 6793–6796.
- (37) Liu, H.; Zhang, H.; Wang, H.; Huang, X.; Huang, G.; Wu, J. Weldable, Malleable and Programmable Epoxy Vitrimers with High Mechanical Properties and Water Insensitivity. *Macromolecules* **2019**, 1 (7), 6789–6799.
- (38) Demongeot, A.; Groote, R.; Goossens, H.; Hoeks, T.; Tournilhac, F.; Leibler, L. Cross-Linking of Poly(Butylene Terephthalate) by Reactive Extrusion Using Zn(II) Epoxy-Vitrimer Chemistry. *Macromolecules* **2017**, 50 (16), 6117–6127.
- (39) Furlán, R. L. E.; Mata, E. G.; Mascaretti, O. A. Butylstannonic Acid Catalyzed Transesterification of Carboxylic Esters. *Tetrahedron Lett.* **1998**, 39 (16), 2257–2260.
- (40) Mascaretti, O. A.; Furlán, R. L. E.; Salomon, C. J.; Mata, E. G. Recent Applications of Organotin Oxides/Hydroxides and Alkylstannonic Acids in Organic Synthesis. *Phosphorus, Sulfur Silicon Relat. Elem.* **1999**, 150–151, 89–97.
- (41) Noda, M. Organotin(IV) Compounds as Intramolecular Transesterification Catalysts in Thermal Depolymerization of Poly(L-Lactic Acid) Oligomer to Form LL-Lactide. *Prep. Biochem. Biotechnol.* **1999**, 29 (4), 333–338.

- (42) Casas, A.; Ramos, M. J.; Rodríguez, J. F.; Pérez, Á. Tin Compounds as Lewis Acid Catalysts for Esterification and Transesterification of Acid Vegetable Oils. *Fuel Process. Technol.* **2013**, *106*, 321–325.
- (43) Du, Z.; Kang, W.; Cheng, T.; Yao, J.; Wang, G. Novel Catalytic Systems Containing N-BuSn(O)OH for the Transesterification of Dimethyl Carbonate and Phenol. *J. Mol. Catal. A Chem.* **2006**, *246* (1–2), 200–205.
- (44) Brito, Y. C.; Ferreira, D. A. C.; Fragoso, D. M. D. A.; Mendes, P. R.; Oliveira, C. M. J. D.; Meneghetti, M. R.; Meneghetti, S. M. P. Simultaneous Conversion of Triacylglycerides and Fatty Acids into Fatty Acid Methyl Esters Using Organometallic Tin(IV) Compounds as Catalysts. *Appl. Catal. A Gen.* **2012**, *443–444*, 202–206.
- (45) Lee, H.; Kim, S. J.; Ahn, B. S.; Lee, W. K.; Kim, H. S. Role of Sulfonic Acids in the Sn-Catalyzed Transesterification of Dimethyl Carbonate with Phenol. *Catal. Today* **2003**, *87* (1–4), 139–144.
- (46) Serra, T. M.; De Mendona, D. R.; Da Silva, J. P. V.; Meneghetti, M. R.; Plentz Meneghetti, S. M. Comparison of Soybean Oil and Castor Oil Methanolysis in the Presence of Tin(IV) Complexes. *Fuel* **2011**, *90* (6), 2203–2206.
- (47) Davies, G. A.; Gielen, M.; Pannell, K.; Tiekink, E. *Tin Chemistry, Fundamentals, Frontier, And Application*; 2008.
- (48) Safronov, A.; Somova, T.; Suvorova, A.; Fisch, M. H.; Stewen, U.; Bacaloglu, R.; Dooley, T. Mechanism of Organotin Stabilization of Poly(Vinyl Chloride). 6. Compatibility of Organotin Stabilizers with PVC. *J. Vinyl Addit. Technol.* **2003**, *9* (3), 127–137.
- (49) Yousif, E. A Review of Organotin Compounds: Chemistry and Applications. *Arch. Org. Inorg. Chem. Sci.* **2018**, *3* (3), 344–352.
- (50) Ali, M. M.; A., E.-H. G.; Emad, Y. Photostabilizing Efficiency of PVC in the Presence of Organotin as Phoyostabilizers. *Molecules* **2016**, *21*, 1151.
- (51) Meneghetti, M. R.; Meneghetti, S. M. P. Sn(IV)-Based Organometallics as Catalysts for the Production of Fatty Acid Alkyl Esters. *Catal. Sci. Technol.* **2015**, *5* (2), 765–771.
- (52) Da Silva Mônica A.; Neto, A. S. S. dos S. A. J. S.; Giertyas, C. J.; Bortoluzzi, J. H.; Meneghetti, M. R.; Meneghetti, S. M. P. Evaluation of Esterification of Oleic Acid and Glycerol in the Presence of Organotin IV Compounds. *Eur. J. lipid Sci. Technol.* **2019**, *121*.
- (53) Liu, W.; Schmidt, D. F.; Reynaud, E. Catalyst Selection, Creep, and Stress Relaxation in High-Performance Epoxy Vitrimers. *Ind. Eng. Chem. Res.* **2017**, *56* (10), 2667–2672.
- (54) ASTM (D638-02a). American Society for Testing and Materials. Standard Test Method for Tensile Properties of Plastics (D 638 - 02a) - SCAN VERSION. *Astm* **2003**, *08*, 46–58.
- (55) ASTM D5045–14. Standard Test Methods for Plane-Strain Fracture Toughness and Strain Energy Release Rate of Plastic Materials. *ASTM Int.* **2014**, 1–9.

- (56) Gershevitz, O.; Sukenik, C. N. In Situ FTIR-ATR Analysis and Titration of Carboxylic Acid-Terminated SAMs. *J. Am. Chem. Soc.* **2004**, *126* (2), 482–483.
- (57) Mustata, F.; Tudorachi, N. Thermal Behavior of Epoxy Resin Cured with Aromatic Dicarboxylic Acids. *J. Therm. Anal. Calorim.* **2016**, *125* (1), 97–110.
- (58) Matějka, L.; Pokorný, S.; Dušek, K. Acid Curing of Epoxy Resins. A Comparison between the Polymerization of Diepoxide-diacid and Monoepoxide-cyclic Anhydride Systems. *Die Makromol. Chemie* **1985**, *186* (10), 2025–2036.
- (59) Montarnal, D.; Tournilhac, F.; HIDALGO, M.; Leibler, L. Epoxy-Based Networks Combining Chemical and Supramolecular Hydrogen-Bonding Crosslinks. *J. Polym. Sci. Part A Polym. Chem.* **2009**, *46* (April), 1133–1141.
- (60) Fabris, H. J.; Knauss, W. G. Synthetic Polymer Adhesives. *Compr. Polym. Sci. Suppl.* **1989**, 131–177.
- (61) Matějka, L.; Chabanne, P.; Tighzert, L.; Pascault, J. P. Cationic Polymerization of Diglycidyl Ether of Bisphenol A. *J. Polym. Sci. Part A Polym. Chem.* **1994**, *32* (8), 1447–1458.
- (62) Blank, W.; He, Z. Catalysis of the Epoxy-Carboxyl Reaction. *Int. Waterborne, High-Solids* **2001**, *74* (926), 33–41.
- (63) Flory, P. J. Kinetics of Polyesterification: A Study of the Effects of Molecular Weight and Viscosity on Reaction Rate. *J. Am. Chem. Soc.* **1939**, *61* (12), 3334–3340.
- (64) Yang, Y.; Peng, G.; Wu, S.; Hao, W. A Repairable Anhydride-Epoxy System with High Mechanical Properties Inspired by Vitrimers. *Polymer (Guildf)*. **2018**, *159* (October), 162–168.
- (65) Edholm, O.; Blomberg, C. Stretched Exponentials and Barrier Distributions. *Chem. Phys.* **2000**, *252* (1–2), 221–225.
- (66) Ricarte, R.; Shanbhag, S. Unentangled Vitrimer Melts: Interplay between Chain Relaxation and Cross-Link Exchange Controls Linear Rheology. *ChemRxiv* **2020**, *54* (7), 3304–3320.
- (67) Winne, J. M.; Leibler, L.; Du Prez, F. E. Dynamic Covalent Chemistry in Polymer Networks: A Mechanistic Perspective. *Polym. Chem.* **2019**, *10* (45), 6091–6108.
- (68) Wu, S. Control of Intrinsic Brittleness and Toughness of Polymers and Blends by Chemical Structure: A Review. *Polym. Int.* **1992**, *29* (3), 229–247.